Gradient in the climate change signal of European discharge predicted by a multi-model ensemble

Stefan Hagemann and Daniela Jacob

Max Planck Institute for Meteorology, Bundesstr.53, 20146 Hamburg, Germany

Tel.: +49 40 41173 101, Fax: +49 40 41173 366, email: Hagemann@dkrz.de

Abstract

In order to perform hydrological studies on the PRUDENCE regional climate model (RCM) simulations, a special focus was put on the discharge from large river catchments located in northern and central Europe. The discharge was simulated with a simplified land surface (SL) scheme and the Hydrological Discharge (HD) model. The daily fields of precipitation, 2m temperature and evapotranspiration from the RCM simulations were used as forcing. Therefore the total catchment water balances are constrained by the hydrological cycle of the different RCMs. The validation of the simulated hydrological cycle from the control simulations shows that the multi-model ensemble mean is closer to the observations than each of the models, especially if different catchments and hydrological variables are considered. Therefore, the multi-model ensemble mean can be used to largely reduce the uncertainty that is introduced by a single RCM. This also provides more confidence in the future projections for the multi-model ensemble means. The scenario simulations predict a gradient in the climate change signal over Northern and Central Europe. Common features are the overall warming and the general increase of evapotranspiration. But while in the northern parts the warming will enhance the hydrological cycle leading to an increased discharge, the large warming, especially in the summer, will slow down the hydrological cycle caused by a drying in the central parts of Europe which is accompanied by a reduction of discharge. The comparison of the changes predicted by the multi-model ensemble mean to the changes predicted by the driving GCM indicates that the RCMs can compensate problems that a driving GCM may have with local scale processes or parameterizations.

1. Introduction

Ten regional climate models (RCMs) participated in the PRUDENCE (Christensen and Christensen, 2006) project. In the present study the RCM simulations conducted at a horizontal resolution of about 50 km were used (see Jacob et al. 2006 for details of the models). The lateral boundary conditions for all RCMs were provided by the GCM HadAM3H (see Buonomo et al., 2006 for details) and the lower (sea-surface) boundary conditions were taken from observations and HadCM3 (see Rowell 2005 for details). A few RCMs have used a slightly different setup within PRUDENCE. ARPEGE is a global model with a stretched grid that does not require lateral boundary fields (see, e.g., Déqué et al., 2005), and therefore only uses the SST as climate forcing. The RCM HadRM3P uses boundary conditions obtained with HadAM3P (Jones et al., 2004), which is a slightly modified version of the atmospheric GCM HadAM3H. All models have been run for a control period, 1961-1990, and a future scenario period, 2071-2100, following the A2 emission scenario from IPCC (Nakicenovic et al., 2000).

We have performed hydrological studies on all RCM simulations, thereby focussing on the discharge from large European rivers. The discharge was simulated with the Hydrological Discharge (HD) model (Hagemann and Dümenil Gates, 2001). The technical methods to calculate the discharge from the RCM simulations are described in Section 2. Section 3 deals with the validation of the simulated hydrological cycle of the control simulations, Section 4 considers the results of the scenario simulations, and Section 5 gives some conclusions.

It has to be noted that in this study only one scenario was considered, and only forcing from one GCM simulation was used. Especially individual GCMs provide a wide spectrum of results and thereby each single GCM introduces larger uncertainties into the RCM results. In our study we focus (along the lines of the PRUDENCE project) on how the uncertainties of RCMs can be reduced by a multi-model ensemble, and on the results obtained by the multi-model ensemble mean using the common forcing of one GCM. Therefore the results of this study are preliminarily conditional on the choice of the GCM HadAM3H. These results will be further enhanced and expanded by results from the forthcoming European Union project ENSEMBLES that started in September 2004, which will deal with RCM predictions using different scenarios and different GCM forcings.

2. Methods

The HD model (Hagemann and Dümenil Gates, 2001) is used to simulate the discharge from the model output of 10 RCMs. It is a state of the art discharge model that is applied and validated on the global scale, and it is also part of the coupled atmosphere-ocean GCM ECHAM5/MPI-OM (Latif et al., 2003). It globally simulates the lateral freshwater fluxes at the land surface. As a general strategy the HD model computes the discharge at 0.5°

resolution using a daily time step. In the HD model, the lateral waterflow is separated into the three flow processes of overland flow, baseflow and riverflow. Overland flow uses surface runoff as input and is representing the fast flow component within a gridbox, baseflow is fed by drainage from the soil and represents the slow flow component, and the inflow from other gridboxes contributes to riverflow. The sum of the three flow processes equals the total outflow from a gridbox. The model parameters are functions of the topography gradient between gridboxes, the slope within a gridbox, the gridbox length, the lake area and the wetland fraction of a particular gridbox.

As mentioned above, the HD model uses daily fields of surface runoff and drainage from the soil as input to represent fast and slow flow processes. Practically, only total runoff has been delivered to the PRUDENCE database located at DMI. Thus, it was necessary to perform additional analyses to partition total runoff into components that represent fast and slow responses. This is done with a simplified land surface (SL) scheme (Hagemann and Dümenil Gates, 2003) which uses daily fields of precipitation and 2m temperature to simulate the hydrological processes at the land surface. The SL scheme incorporates the main components of the hydrological cycle at the land surface and primarily uses relations that are functions of temperature and precipitation. A more detailed description is given by Hagemann and Dümenil Gates (2003). For the current study two slight modifications have been implemented. Drainage is calculated according to Clapp and Hornberger (1978), and in the daily degree formula to calculate the snowmelt (Bergström, 1992) a sinusoidal correction is applied to the degree melting factor. In order to constrain the total water balance by the hydrological cycle of the different RCMs, a special version of the SL scheme is used which additionally uses the RCM evapotranspiration as input. This is different from other hydrological approaches applied within the PRUDENCE project where the water balance is corrected and evapotranspiration is calculated by the hydrological model (Graham et al., 2006).

Usually the SL scheme is applied at the same horizontal resolution as the corresponding input data. In the PRUDENCE database, all daily RCM simulation data are available only on their original model grid, which is different in each of the models. In order to use the same SL scheme configuration for all RCMs the original RCM data were interpolated to the same regular 0.5º grid that is also directly used by the HD model. Note that no height correction is conducted, but as only integrated values over large catchments are considered in the following, biases introduced by a different orography at specific gridpoints between the original RCM grid and the regular 0.5º grid can be neglected.

2.1 Simulation of discharge from REMO with and without the SL scheme

Figure 1 shows the discharge for the Baltic Sea catchment (from its land area into the sea), the Danube and the Rhine simulated with the HD model by directly using surface runoff and drainage from the REMO control simulation, and by using the corresponding fields calculated with the SL scheme from REMO precipitation, evapotranspiration and 2m temperature. The main differences between both simulated discharges can be seen in the spring flow due to different handling of snow processes in REMO and the SL scheme, especially with regard to the timing of the snowmelt. For the Rhine it seems that the simplified process formulations in the SL scheme have problems to accurately represent the complex snow processes in the Alpine part of the Rhine catchment, thereby causing a delayed peak of discharge (pale solid line). This seems to be adequately simulated by REMO as the simulated discharge (pale dashed line) is close to the observed discharge (dark solid line). But for the Danube and the Baltic Sea catchment, the SL scheme yields an improved simulated discharge compared to the direct use of the REMO surface runoff and drainage. This indicates that the accuracy of the SL scheme is within the quality range of land surface schemes used in RCMs.

3. Validation of the hydrological cycle in the control simulations

In order to evaluate the simulated discharge, a validation of the simulated hydrological cycle was performed. Here, several large European catchments are considered (Figure 2), i.e. the Baltic Sea catchment (land points only are considered in the following if not stated otherwise) representing a maritime climate (about 1.8 Million km^2), the Danube catchment representing a continental climate (about 800000 km^2), and the Rhine catchment (about 160000 km^2) that is located in a transition zone of both climates. The latter is also largely influenced by Alpine snow processes and climate. The validation focused on common RCM model problems, such as those investigated by Hagemann et al. (2004) for several RCM simulations driven by data from the 15 years re-analysis of ECMWF (ERA15; Gibson et al., 1997) [ARPEGE (using the same simulation as in the present study which is driven only by observed SST), CHRM, HadRM3H (Jones et al., 1995; very similar to HadRM3P), HIRHAM, REMO]. These problems comprise the overestimated precipitation in winter and spring over the Baltic Sea catchment and the summer drying problem over the Danube catchment.

3.1 Annual means

Figure 3 compares the annual mean precipitation of all RCMs, their multi-model mean and observations as well as of the driving GCM HadAM3H. Observations are the mean of CMAP (Xie and Arkin, 1997) and GPCP (Huffman et al., 1997) precipitation data. CMAP precipitation data are not corrected for the systematic undercatch of precipitation gauges, which is especially significant for snowfall. For GPCP data, a correction has been applied which is known to be overestimated by a factor of about 2 (Rudolf and Rubel, 2005) so that the actual precipitation amounts are expected to be in between GPCP and CMAP. Figure 3 shows that the multi-model mean is relatively close to the observed precipitation for all catchments, while the different RCMs are distributed around this mean. Here, some models seem to have general dry (CHRM, PROMES) or wet (CLM, RegCM) precipitation biases but usually the biases are catchment specific. The precipitation simulated by the driving GCM HadAM3H is relatively close but slightly larger than the observations in all catchments. (PROMES and RegCM are not considered for the Baltic Sea catchment as their model domains do not include the whole catchment.)

The multi-model mean of evapotranspiration is relatively close to the observed annual mean evapotranspiration (Figure 4) that was calculated from the difference of the mean observed precipitation (mean of CMAP and GPCP data) minus the observed climatological discharge. The spread around the mean is comparable to the spread for precipitation. A strong negative bias is found for PROMES, which is related to a very small soil water holding capacity used in its soil scheme. Here, the soil dries too fast so that evapotranspiration cannot be maintained for longer dry periods. Relatively high positive evapotranspiration biases apply to REMO, HIRHAM and RegCM. The GCM HadAM3H is overestimating the evapotranspiration in all catchments.

Figure 5 shows how the biases in precipitation and evapotranspiration add together in the runoff that is equal to P-E in the long-term annual mean. Here, the spread around the mean is somewhat larger than for precipitation and evapotranspiration, but the multi-model means are still relatively close to the observed values. Noticeable are the general dry biases of HIRHAM and CHRM and the wet biases of CLM, PROMES and RegCM. For HadAM3H, the wet biases in precipitation and evapotranspiration are compensating each other, therefore the simulated P-E agrees well with the observed discharges.

3.2 Monthly means

Figure 6 shows the simulated and observed mean annual cycles of precipitation. For the Baltic Sea catchment, the common model bias of too much precipitation in the winter and spring becomes visible in the deviation of the multi-model ensemble mean from the two observations of CMAP and GPCP. As mentioned in Section 3.1, the actual precipitation amounts are expected to be in between GPCP and CMAP. For the Danube catchment, the prominent summer drying shows up in the multi-model ensemble mean. An overestimation of precipitation in the spring can be seen for all three catchments. For the Rhine a small drying problem seems to occur in September. Despite of the common biases the general shape of the multi-model mean follows quite closely the observed curves.

The simulated mean annual cycle of evapotranspiration is compared to ERA15 data in Figure 7. Even with the uncertainty in the ERA15 evapotranspiration (cf. Hagemann et al., 2004), the multi-model mean agrees quite well with the ERA15 data for the catchments of the Baltic Sea and the Rhine. Over the Danube catchment the summer drying problem causes too dry soils and, thus, a general dry bias of evapotranspiration in the summer.

As the general dry biases in summer precipitation and evapotranspiration are compensating each other, the summer drying does now show up in the simulated discharge shown in Figure 8. The general overestimation of precipitation in spring causes a delay in the spring peak of discharge in the multi-model mean. A part of the delayed peak of the Rhine discharge is caused by the problems the SL scheme has in representing the complex snow processes in the Alpine part of the Rhine catchment (see Sect. 2.1).

In summary it can be stated that a large spread exists between the simulated hydrological variables of the 10 RCMs. But on the average the multi-model ensemble mean is usually closer to the observations than each of the models, especially if several catchments and different hydrological variables are considered. The fact that the multi-model ensemble mean is close to the observations as well as to the HadAM3H simulation may raise speculations on a possible too strong forcing from the GCM, which can be declined. If the forcing would be so dominant a much narrower spread in the RCM simulations should be expected, and the different RCM simulations would be much closer to the HadAM3H simulation. But this is not the case, which indicates that the forcing is not strong enough to automatically force all driven RCMs to be close to the HadAM3H simulation.

In a perfect GCM-RCM coupling environment, the RCM results should be close to the GCM results only in areas and times where the weather patterns are dominated by the large-scale circulation. The RCMs are constructed to represent the reality. In order to do this each RCM uses different parameterizations, dynamical and physical packages, so that each RCM has different distributions of errors and biases. The use of different RCMs to simulate the climate over a certain region is similar to the measurement of a specific variable where the measurement instrument has certain error. For the latter the mean of several measurements is expected to be close to the real value of the measured quantity. Analogous it can be expected that the multi-model ensemble mean is close to the observed climate, despite errors entering the RCM simulation through the lateral boundaries and despite common model problems.

4. Future changes in the A2 scenario simulations

Figure 9 shows the simulated future changes in the annual mean precipitation over the catchments of the Baltic Sea, Danube and Rhine. For the Baltic Sea catchment and the Danube catchment, most RCMs agree well in the direction of the change. For the first, the multi-model ensemble mean predicts an increase of about +10%, and a reduction of about -5% for the second. The model signal is quite undetermined for the Rhine catchment, so that the multi-model ensemble mean predicts almost no change. With regard to evapotranspiration (Figure 10), clear increases are predicted for the Baltic Sea (about +13%) and Rhine (about +7%) catchments. HadRM3P is an outlier and predicts a reduction in evapotranspiration for the Rhine catchment. For the Danube catchment, the RCMs vary in their predictions so that almost no change is yielded in the multi-model mean. The changes in precipitation P and evapotranspiration E add up together in the change in P-E (equals runoff in the long-term annual mean) shown in Figure 11. For the Baltic Sea catchment, the RCMs differ in their signal resulting in a small increase of about +4% in the multi-model mean. For the Danube and the Rhine catchment, all RCMs agree well in their reduction signal, predicting mean reductions of about -16% and -11%, respectively.

While the annual mean hydrological values simulated by the GCM HadAM3H for the control period were close to the multi model ensemble mean of the RCMs, the predicted changes of the A2 scenario simulation differ clearly in some cases. Generally HadAM3H predicts less increases of precipitation and evapotranspiration where the majority of RCMs predict a rise, and more decreases where the RCMs tend to predict a reduction. This causes larger differences to the multi-model ensemble mean of the RCMs over the Baltic Sea catchment for precipitation (Figure 9), over all catchments for evapotranspiration (Figure 10), and over the Danube and the Rhine catchment for P-E (Figure 11).

While the mean annual temperature increase in all catchments is about 4 °C (±0.5 °C), its seasonal distribution (Figure 12) is geographically varying. Over the Baltic Sea catchment (Figure 12a), one maximum of temperature change is obtained by the multi-model ensemble mean, which is predicted for the winter (January). But over the Danube (Figure 12b) and the Rhine catchment (similar changes as for Danube, see Graham et al., 2006) two maxima of temperature change are predicted that are located in the winter (December) and summer (August). Here, the winter maximum is less pronounced than the summer maximum.

The model spread around the mean temperature signal is relatively narrow, only HadRM3P deviates significantly from the other models over all three catchments, especially in the summer. This is also the case for the GCM HadAM3H, which generally shows a larger warming than the multi model ensemble mean throughout the year over the all three catchments. This points to a common particular model behavior of the HadM3 model family that becomes visible especially during the summer and the neighboring seasons. One possible reason may be that both models tend to simulate too high extreme temperatures and temperature variability in the summer in the control simulations (see, e.g., Lenderink et al., 2006), which results from a lack of evaporative damping due to insufficient soil moisture (Jones, personal communication, 2004). This may impact the climate response of these variables (and probably precipitation).

The model spread over the Baltic Sea catchment is much smaller than over the Danube and Rhine catchments. In the maritime climate of the Baltic Sea catchment, the predicted temperature changes and their variations seem to be mainly related to changes in the large scale atmospheric circulation that enter the RCM model domains by SST changes and atmospheric transport through the lateral boundaries. As this forcing is the same for all RCMs the temperature spread is very small. For the more continental climate over the Danube and the Rhine catchment, the predicted changes are much more influenced by local processes within the model domain so that different RCM formulations representing these processes lead to a larger spread.

In the predicted monthly precipitation signals (Figure 13), a gradient in the signal becomes obvious. Over the Baltic Sea catchment (Figure 13a) a significant precipitation increase is predicted for the winter half of the year (October-March) while the changes remain comparatively weak in the summer half (April-September), except for two peak changes in May (+13%) and September (-13%). For the catchments of Danube (Figure 13b) and Rhine (see Graham et al., 2006), an increase is predicted only for the late winter (January-March). In addition a significant decrease of precipitation is predicted in the summer. Again all models show a very similar signal with some spread around the multi-model ensemble mean that is smallest over the Baltic Sea catchment and in the winter over all catchments. Over the Baltic Sea catchment, REMO is an exception, which is related to a strong sensitivity of its simulated precipitation to too warm Baltic Sea temperatures. In REMO, the lake SST is derived from the SST of the closest sea gridboxes. For the Baltic Sea, an intense summer warming of the SST is predicted by the HadCM3 model (see Sect 1) that turned out to be relatively large (about 7 K warmer than in the current climate; Jacob et al., 2006). Déqué et al. (2006) stated that this behaviour can be considered as erroneous or at least exaggerated, and is caused by the lack of realism of the Baltic Sea in the driving low-resolution coupled simulation. For this reason, SMHI has used a version of its RCM that is coupled to a Baltic Sea ocean model so that the Baltic Sea SSTs were simulated by its ocean component (RCAO; Räisänen et al., 2002). HadAM3H predicts a stronger reduction of precipitation during the summer than the multi model ensemble mean for all three catchments. Again, HadRM3P shows a similar behavior during the summer, where reduction in precipitation is even more pronounced than HadAM3H for the catchments of Danube and Rhine.

With regard to the mean monthly evapotranspiration changes (Figure 14), the largest increase is predicted in the winter for each of the three catchments. Over the Baltic Sea catchment (Figure 14a) an evapotranspiration increase is predicted throughout the year. This is not the case for the other two catchments where evapotranspiration in the summer remains almost unchanged (less than 6%) in the predicted multi-model mean change (Rhine, see Graham et al., 2006), or is even reduced (Danube, Figure 14b). Under wet conditions, such as in the winter and also in the northern summer, the warming enhances the evapotranspiration. But over Central Europe the large summer warming causes a drying of the area. The dried soil cannot satisfy the increased demand of moisture of the warmer atmosphere, which then leads to a reduction of evapotranspiration, thereby counteracting against the increased atmospheric demand. Over the Danube, the impact of the drying is even stronger than the influence of the increased atmospheric demand. Over the Danube and Rhine catchments, the seasonal cycle of change predicted by PROMES is largely deviating from the other RCMs. This is probably related to the relatively small soil moisture storage capacities in its land surface scheme (see Sect. 3.1). Small increases in precipitation may directly lead to increases in evapotranspiration in medium or dry conditions while in wet conditions the evapotranspiration will be almost insensitive to smaller variations in precipitation. For the GCM HadAM3H as well as for HadRM3P, the stronger reduction of summer precipitation leads to an enhanced drying of the catchments thereby causing a more pronounced reduction (or less increase for the Baltic Sea catchment, respectively) of summer evapotranspiration than the other RCMs.

The different changes in precipitation and evapotranspiration lead to pronounced seasonal signals in predicted discharge shown in Figure 15. For the Baltic Sea catchment (Figure 15a), an increase of discharge of about 20% is predicted in the winter and early spring. During the rest of the year no significant change is simulated despite a small reduction of about 10% in June. For the Danube (Figure 15b) and Rhine (Figure 15c), similar changes are simulated where a discharge increase is predicted only in the late winter. The more prominent signal for these two rivers is the decrease of discharge of about 20% in the rest of the year. As for precipitation and evapotranspiration, the predicted climate change responses in the discharge are comparatively robust. Only for the Baltic Sea catchment in the summer is there larger uncertainty in the direction of a possible change. Here, the large change in discharge simulated by REMO is directly linked to the probably overestimated change in precipitation caused by the too warm Baltic Sea SSTs (see above).

Although the GCM HadAM3H predicted stronger reductions in summer precipitation and evapotranspiration than the multi-model ensemble mean, the predicted changes in the monthly discharge are similar to the multi model ensemble mean for the Danube and Rhine catchments, except for somewhat smaller reductions in the summer. For the Baltic Sea catchment, the larger reduction of precipitation predicted in the summer causes a reduction in summer discharge that is stronger than predicted by all RCMs.

In climate change modeling it is commonly assumed that the systematic climate model biases are the same in the control and scenario simulations. Therefore these biases do not appear if only changes between scenario and control simulation are considered. This assumption is supported by Figure 16, which shows that the spread in the predicted discharge changes is much smaller than the model spread of the discharge in the control simulations for all catchments. This indicates that even with the large differences between the RCM discharges of the control simulations, the A2 climate change signal is very much confined and similar for almost all of the models. Thus, the spread of the changes is an indicator of the different climate change sensitivities of the RCMs while the spread around the multi-model ensemble mean of the control simulations is an indicator for the different systematic biases of the RCMs.

5. Conclusions

An ensemble of 10 RCMs was used to conduct climate simulations for current and future climate conditions under the assumption of the A2 scenario. The validation of the simulated hydrological cycle in the current climate has shown that a large spread exists between the models, but that the multi-model ensemble mean can be used to reduce uncertainty introduced by the use of a single RCM. This reduction can be achieved since the multi-model ensemble mean is usually closer to the observations than each of the models, especially if several catchments and hydrological variables are considered. Significant deviations of the ensemble mean to the observations point to common model problems, such as the prominent summer drying problem over Central Europe (Hagemann et al., 2004). Despite of the large differences in the control simulations of the RCMs, where the performance of the RCMs is different over the diverse catchments, the A2 climate change signal is very much confined and similar for almost all of the models. And even those RCMs who particularly disagree with regard to P and E in the control simulations, the A2 signal in the discharge is largely constrained by each of the models. This provides some confidence in the future projections even if only a few of the 10 RCMs are considered. The results also indicate that the changes over the maritime Baltic Sea catchment are mainly related to changes in the large-scale circulation, while over the more continental catchments of Danube and Rhine the effect of local scale processes seems to be more important.

The following changes are predicted by the multi-model ensemble mean. For the Baltic Sea catchment, the precipitation will increase in the winter half of the year (October-March), and evapotranspiration will increase during the whole year with a maximum increase in the winter. These rises in precipitation and evapotranspiration will lead to an increase in discharge (>20%) only in the winter and early spring. The signals for the Danube and Rhine catchments are relatively similar. The precipitation will increase in the late winter (January-March) and decrease in the summer. The evapotranspiration will rise during the whole year, except for the summer, with a maximum increase in the winter. For the Danube, even a decrease is predicted in the summer. In both catchments, these changes lead to a large reduction (>20%) in the discharge throughout the year except in the late winter. Here increases of about 10% are predicted. It seems that the large summer warming intensifies the drying of the Central European area represented by both catchments. These results show that a strong gradient in the climate change signal is predicted by the RCMs. The future warming is intensifying the hydrological cycle in the north of Europe while over Central Europe the warming causes a weakening.

During the summer, the predicted changes by the GCM HadAM3H and the RCM HadRM3P deviate significantly from the RCM multi-model ensemble mean, especially for temperature, precipitation and evapotranspiration. As this common model behavior of the HadM3 model family seems to be independent of resolution, it is probably related to problems in representing certain local effects that are simulated differently than by the other RCMs. Despite these problems with the driving GCM, almost all RCMs predict consistent changes in the hydrological cycle for all catchments. This indicates that the use of RCMs can compensate problems that a driving GCM might have with the representation of local scale processes or parameterizations. Although this is concluded from the scenario simulations we believe that this is also valid for the current climate. However, due to the relatively accurate performance of the GCM HadAM3H over the considered catchments in the current climate, we cannot show this here. Thus, in addition to the higher resolution, a further added value is obtained by the use of the RCM multi-model ensemble mean compared to the GCM.

It has to be noted that in this study only one scenario was considered, and only forcing from one GCM simulation was used. Results of Déqué et al. (2006) indicated that regarding uncertainty based on several models, the number of GCM forcings involved is at least as important as the number of RCMs, and that it is also necessary to consider several scenarios in the case of southern Europe summer warming. How RCM predictions behave using different scenarios and different GCM forcing will be investigated within the forthcoming European Union project ENSEMBLES that started in September 2004. Here, it will be of interest to determine whether using several RCMs with different GCM forcings actually results in more confidence in the overall results. First results considering two different scenarios and two different GCM forcings were obtained with RCAO (Räisänen et al., 2004) within the PRUDENCE project. Here, the four simulations agree on a general increase in precipitation in northern Europe especially in winter and on a general decrease in precipitation in southern and central Europe in summer, but the magnitude and the geographical patterns of the change differ markedly between the two GCM forcings.

Acknowledgement

This study was supported by funding from the European Union within the PRUDENCE project (contract No. EVK2-2001-00156). We are very grateful to Jens Hesselberg Christensen (DMI), who did a great job in coordinating the PRUDENCE project. We would also like to thank all PRUDENCE members who provided data to the DMI data server, especially Ole Bossing Christensen (DMI), Pier Luigi Vidale (ETH), Enrique Sanchez (UCM), and Xunqiang Bi (ICTP) who helped us to solve problems with the data, as well as Ahmed Qureshi (MPI) for his technical support.

References

Bergström, S.: 1992, 'The HBV model - its structure and applications', *Swedish Meteorological and Hydrological Institute, Rep.* **4**, Norrköping, Sweden.

Buonomo, E., Jones, R.G. , Huntingford, C. and Hannaford, J.: 2005, 'The robustness of high resolution predictions of changes in extreme precipitation for Europe', *Q. J. R. Meteorol. Soc.*, in press.

Christensen, J.H., Christensen, O.B.: 2006, 'A summary of the PRUDENCE model projections of changes in European climate by the end of this century', *Climatic Change***,** provisionally accepted, this issue – part 1.

Clapp, R.B., and Hornberger, G.M.: 1978, 'Empirical Equations for some soil hydraulic properties'. *Water Resour. Res.* **14**, 601-604.

Déqué, M., Jones, R.G., Wild, M., Giorgi, F., Christensen, J.H., Hassell, D.C., Vidale, P.L., Rockel, B., Jacob, D., Kjellström, E., de Castro, M., Kucharski, F., and van den Hurk, B.: 2005, 'Global high resolution versus Limited Area Model scenarios over Europe: results from the PRUDENCE project', *Clim. Dyn.* **25**, 653-670.

Déqué, M., Rowell, D., Schär, C., Giorgi, F., Christensen, J. H., Rockel, B., Jacob, D., Kjellstrom, E., de Castro, M., and van den Hurk, B.: 2006, 'An intercomparison of regional climate models for Europe: assessing uncertainties in model projections', *Climatic Change*, provisionally accepted, this issue - part 1.

Gibson, J.K., Kållberg, P., Uppala, S., Hernandez, A., Nomura, A., and Serrano, E.:1997, ‚Era description' *ECMWF Re-Anal. Proj. Rep. Ser.* **1**, Reading, UK.

Graham, L.P., Hagemann, S., Jaun, S., and Beniston, M.: 2006, 'On interpreting hydrological change from regional climate models', *Climatic Change*, provisionally accepted, this issue - part 1.

Hagemann, S., and Dümenil Gates, L.: 2001, 'Validation of the hydrological cycle of ECMWF and NCEP reanalyses using the MPI hydrological discharge model', *J Geophys Res* **106**, 1503-1510.

Hagemann, S., and Dümenil Gates, L.: 2003, 'Improving a subgrid runoff parameterization scheme for climate models by the use of high resolution data derived from satellite observations', *Clim. Dyn.* **21**, 349-359.

Hagemann, S., Machenhauer, B., Jones, R., Christensen, O.B., Déqué, M., Jacob, D., and Vidale, P.L.: 2004, 'Evaluation of Water and Energy Budgets in Regional Climate Models Applied Over Europe', *Clim. Dyn.* **23**, 547-567.

Huffman, G.J., Adler, R.F., Arkin, A., Chang, A., Ferraro, R., Gruber, A., Janowiak, J., Joyce, R.J., McNab, A., Rudolf, B., Schneider, U. and Xie, P.: 1997, 'The Global Precipitation Climatology Project (GPCP) combined precipitation data set,' *Bull. Amer. Meteor. Soc.* **78**, 5-20.

Jacob, D., Bärring, L., Christensen, O.B., Christensen, J.H., de Castro, M., Déqué, M., Giorgi, F., Hagemann, S., Hirschi, M., Jones, R.G., Kjellström, E., Lenderink, G., Rockel, B., Sánchez, E., Schär, C., Seneviratne, S.I., Somot, S., van Ulden, A., and van den Hurk, B.: 2006, ' An inter-comparison of regional climate models for Europe: Design of the experiments and model performance', *Climatic Change*, submitted, this issue - part 1.

Jones, R.G., Murphy, J.M., and Noguer, M.: 1995, 'Simulation of climate change over Europe using a nested regional climate model. I: Assessment of control climate, including sensitivity to location of lateral boundaries', *Q.J.R. Meteorol. Soc.* **121**, 1413-1449.

Jones, R.G., Noguer, M., Hassell, D.C., Hudson, D., Wilson, S.S., Jenkins, G.J., and Mitchell, J.F.B.: 2004, 'Generating high resolution climate change scenarios using PRECIS', Met Office Hadley Centre, Exeter, UK, p. 35.

Latif, M., Roeckner, E., Botzet, M., Esch, M., Haak, H., Hagemann, S., Jungclaus, J., Legutke, S., Marsland, S., and Mikolajewicz, U.: 2003, 'Reconstructing, monitoring, and predicting decadal-scale changes in the North Atlantic thermohaline circulation with sea surface temperature', *J. Climate* **17**, 1605-1613.

Lenderink, G., van den Hurk, B.J.J.M, van Ulden, A.P., and van Meijgaard, E.: 2006, 'Summertime inter-annual temperature variability in an ensemble of regional model simulations: analysis of the surface energy budget', *Climatic Change*, provisionally accepted, this issue - part 2.

Nakicenovic, N., Alcamo, J., Davis, G., de Vries, B., Fenhann, J., Gaffin, S., Gregory, K., Grübler, A., Jung, T.Y., Kram, T., La Rovere, E.L., Michaelis, L., Mori, S., Morita, T., Pepper, W., Pitcher, H., Price, L., Raihi, K., Roehrl, A., Rogner, H-H., Sankovski, A., Schlesinger, M., Shukla, P., Smith, S., Swart, R., van Rooijen, S., Victor, N., and Dadi, Z.: 2000, 'IPCC Special Report on Emissions Scenarios', Cambridge University Press, Cambridge, United Kingdom and New York, NY, USA.

Räisänen, J., Hansson, U., and Ullerstig, A.: 2002, 'First GCM-driven RCAO runs of recent and future climate', In *SWECLIM Newsletter* **12**, 16-21.

Räisänen, J., Hansson, U., Ullerstig, A., Döscher, R., Graham, L.P., Jones, C., Meier, H.E.M., Samuelsson, P., and Willén, U.: 2004, 'European climate in the late twenty-first century: regional simulations with two driving global models and two forcing scenarios', *Clim. Dyn.* **22**, 13-31.

Rowell, D.P.: 2005, 'A scenario of European climate change for the late 21st century: seasonal means and interannual variability', *Clim. Dyn.*, DOI: 10.1007/s00382-005-0068-6.

Rudolf, B., and Rubel, F.: 2005, 'Global precipitation'. Chapter 11 of Hantel, M., Ed. (2005), Observed Global Climate, Landolt-Boernstein: Numerical Data and Functional Relationships in Science and Technology - New Series, Group 5: Geophysics , Vol. 6, Springer-Verlag, 567 p.

van den Hurk, B., Hirschi, M., Schär, C., Lenderink, G., van Meijgaard, E., van Ulden, A., Rockel, B., Hagemann, S., Graham, P., Kjellström, E., and Jones, R.: 2004, 'Soil control on runoff response to climate change in regional climate model simulations', *J. Climate* **18**, 3536-3551.

Xie, P., and Arkin, P.: 1997, 'Global precipitation: A 17-year monthly analysis based on gauge observations, satellite estimates and numerical model outputs', *Bull. Amer. Meteor. Soc.* **78**, 2539-2558.

Figure Captions

Figure 1 HD model discharge for 1961-1990 simulated using surface runoff and drainage obtained directly from the REMO control simulation (pale dashed line) and calculated with the SL scheme (pale solid line).

Figure 2 Large river catchments of Europe at 0.5º resolution.

Figure 3 Annual means precipitation over the catchments of Baltic Sea, Danube and Rhine. The observed precipitation was calculated from the mean of CMAP and GPCP data.

Figure 4 Annual mean evapotranspiration over the catchments of Baltic Sea, Danube and Rhine. The observed evapotranspiration was calculated from the difference of the mean precipitation (mean of CMAP and GPCP data) minus the observed climatological discharge.

Figure 5 Annual mean P-E over several catchments. The observed runoff (= P-E) corresponds to the observed climatological discharge.

Figure 6 Mean annual cycle of precipitation over the catchments of a) Baltic Sea, b) Danube and c) Rhine. Mean designates the multi-model ensemble mean of the 10 RCMs (8 for the Baltic Sea catchment).

Figure 7 Mean annual cycle of evapotranspiration over the catchments of a) Baltic Sea, b) Danube and c) Rhine. Mean designates the multi-model ensemble mean of the 10 RCMs (8 for the Baltic Sea catchment).

Figure 8 Mean annual cycle of discharge for the a) Baltic Sea catchment, b) Danube and c) Rhine. Mean designates the multi-model ensemble mean of the 10 RCMs (8 for the inflow into the Baltic Sea).

Figure 9 Annual mean changes in precipitation over the catchments of Baltic Sea, Danube and Rhine.

Figure 10 Annual mean changes in evapotranspiration over the catchments of Baltic Sea, Danube and Rhine.

Figure 11 Annual mean changes in P-E (= runoff) over the catchments of Baltic Sea, Danube and Rhine.

Figure 12 Mean monthly 2m temperature changes over the catchments of a) Baltic Sea and b) Danube. Mean designates the multi-model ensemble mean change of the 10 RCMs (8 for the Baltic Sea catchment).

Figure 13 Mean monthly precipitation changes over the catchments of a) Baltic Sea and b) Danube. Mean designates the multi-model ensemble mean change of the 10 RCMs (8 for the Baltic Sea catchment).

Figure 14 Mean monthly evapotranspiration changes over the catchments of a) Baltic Sea and b) Danube. Mean designates the multi-model ensemble mean change of the 10 RCMs (8 for the Baltic Sea catchment).

Figure 15 Mean monthly discharge changes in the a) Baltic Sea catchment, b) Danube and c) Rhine. Mean designates the multi-model ensemble mean change of the 10 RCMs (8 for the Baltic Sea catchment).

Figure 16 Spread around the multi-model ensemble mean discharge for the control simulations (dark curves) compared to the spread of the predicted discharge changes (pale curves) in the Baltic Sea catchment (solid), the Danube (dashed) and the Rhine (dotted). The spread is given relative to the multi-model ensemble mean discharge.

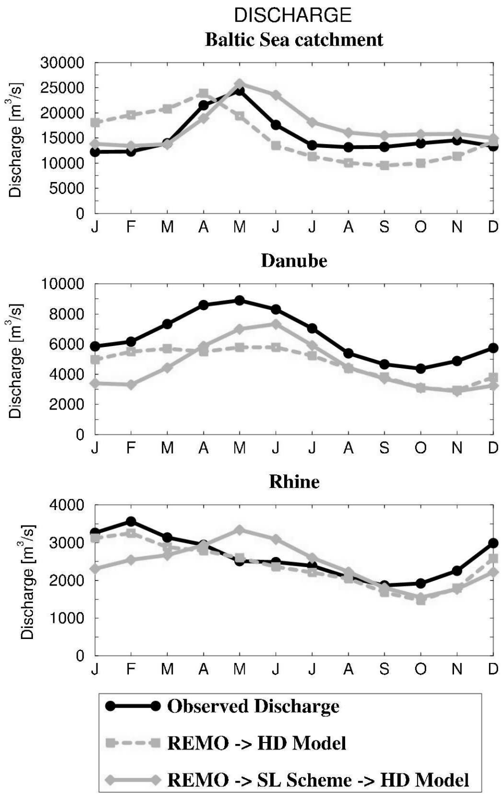

Figure 1 HD model discharge for 1961-1990 simulated using surface runoff and drainage obtained directly from the REMO control simulation (pale dashed line) and calculated with the SL scheme (pale solid line).

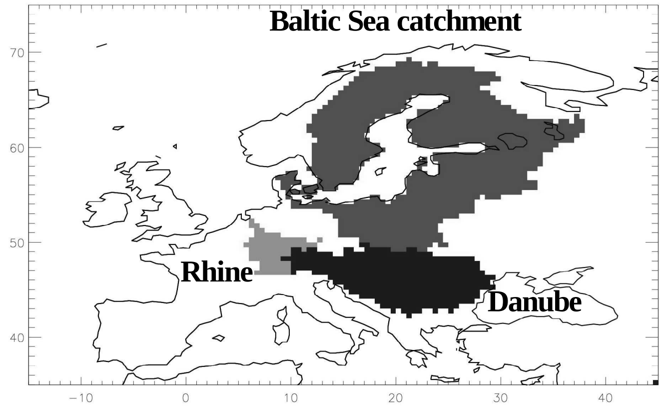

Figure 2 Large river catchments of Europe at 0.5º resolution.

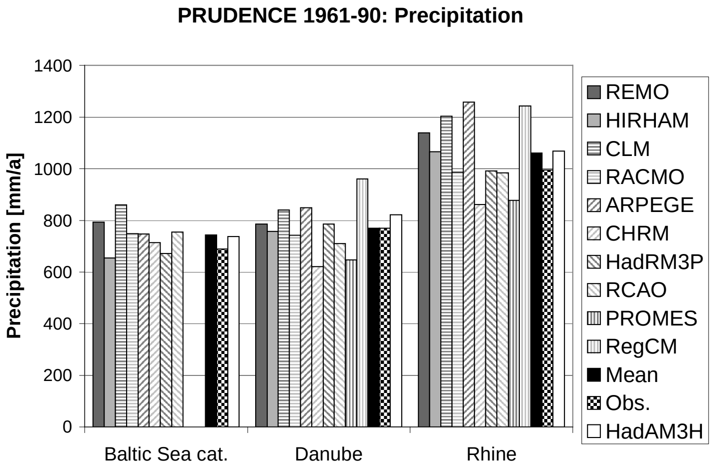

Figure 3 Annual means precipitation over the catchments of Baltic Sea, Danube and Rhine. The observed precipitation was calculated from the mean of CMAP and GPCP data.

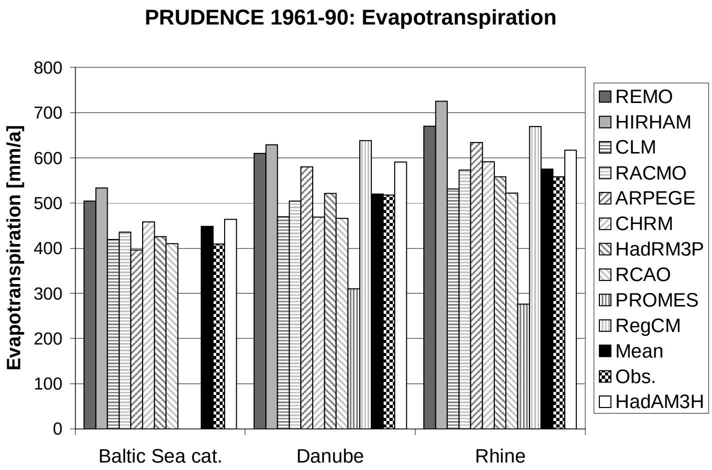

Figure 4 Annual mean evapotranspiration over the catchments of Baltic Sea, Danube and Rhine. The observed evapotranspiration was calculated from the difference of the mean precipitation (mean of CMAP and GPCP data) minus the observed climatological discharge.

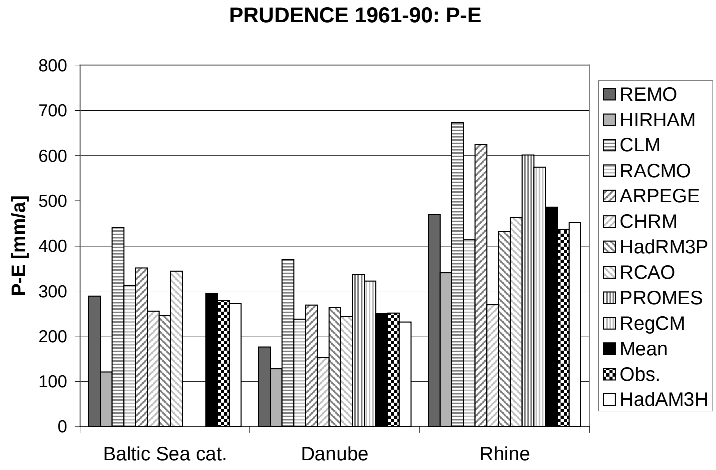

Figure 5 Annual mean P-E over several catchments. The observed runoff (= P-E) corresponds to the observed climatological discharge.

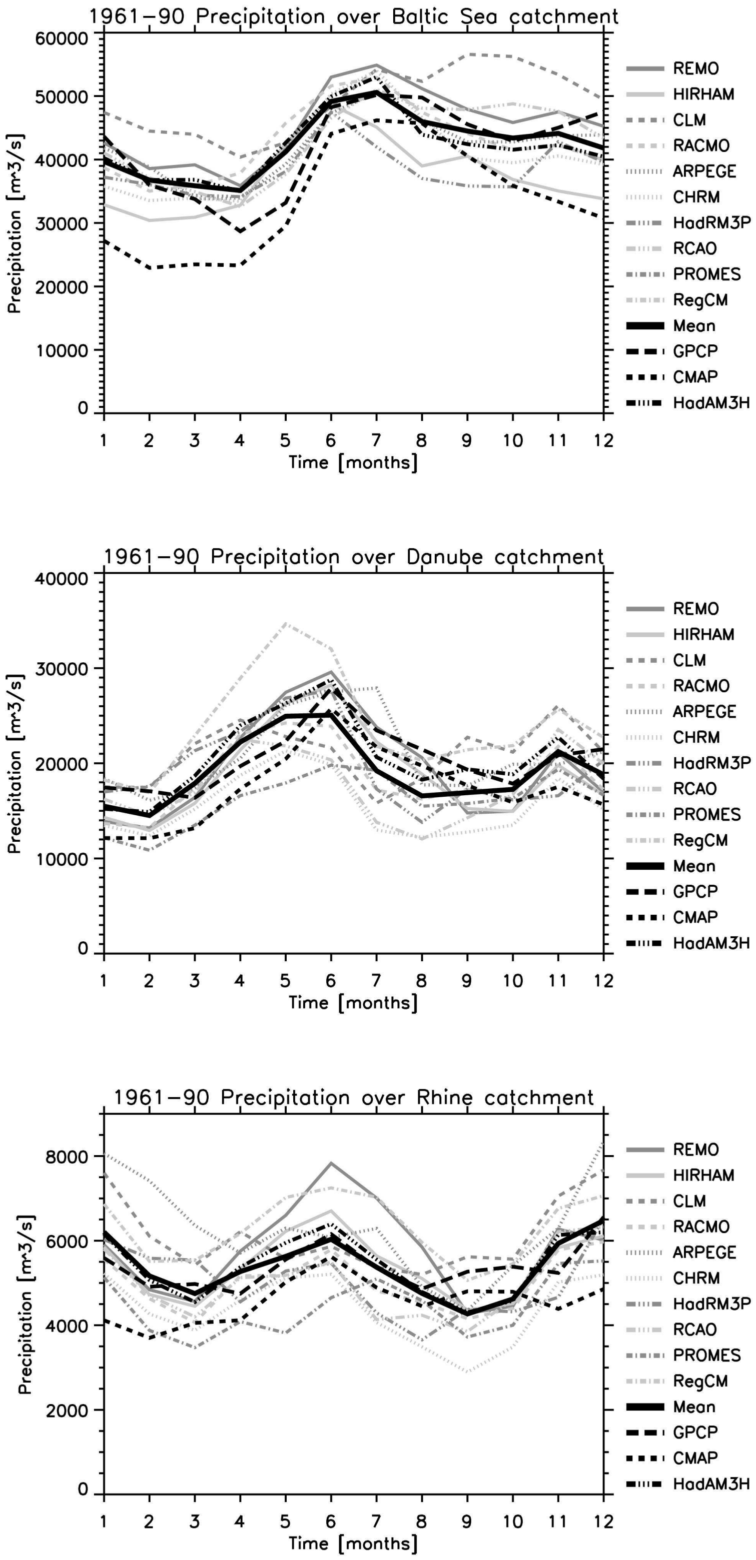

Figure 6 Mean annual cycle of precipitation over the catchments of a) Baltic Sea, b) Danube and c) Rhine. Mean designates the multi-model ensemble mean of the 10 RCMs (8 for the Baltic Sea catchment).

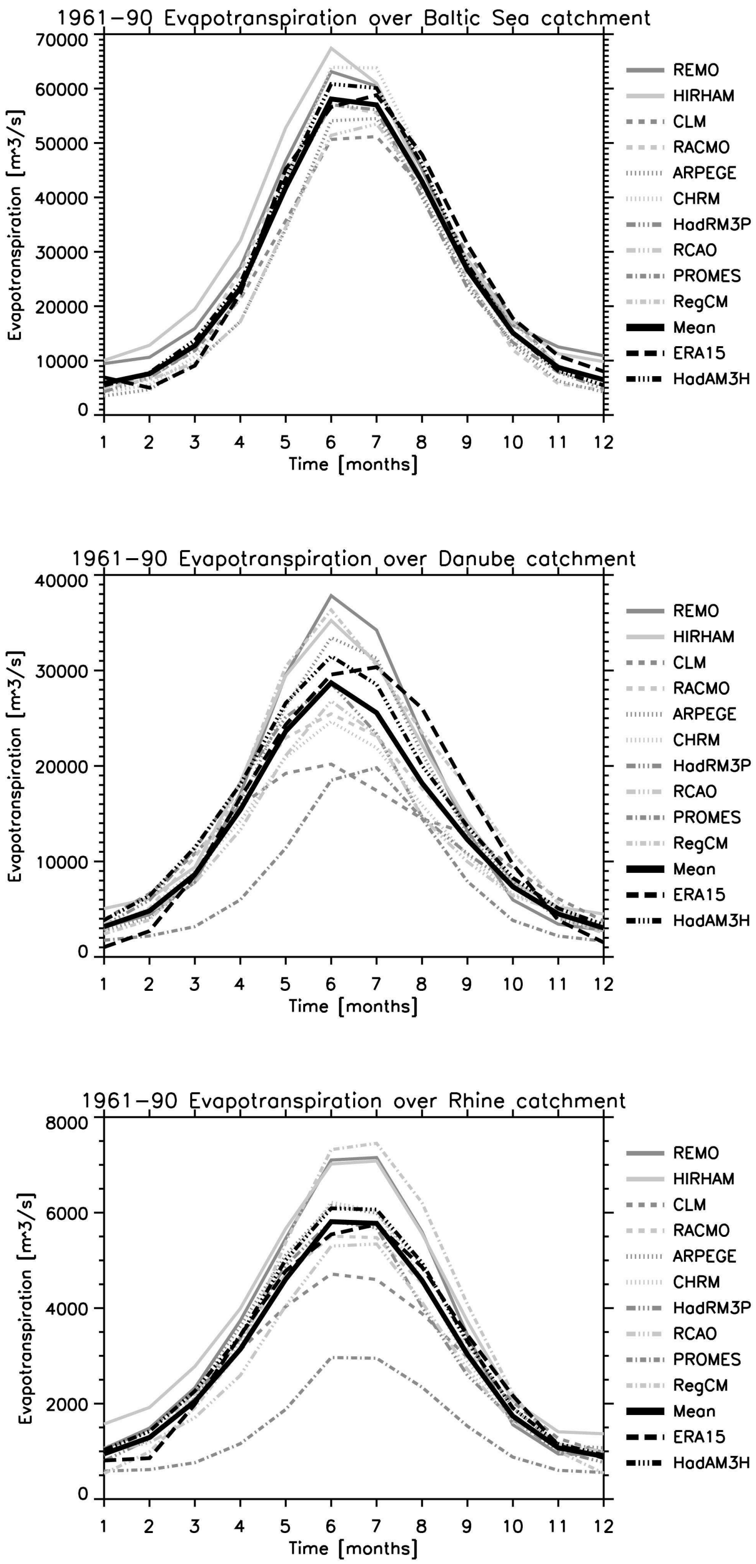

Figure 7 Mean annual cycle of evapotranspiration over the catchments of a) Baltic Sea, b) Danube and c) Rhine. Mean designates the multi-model ensemble mean of the 10 RCMs (8 for the Baltic Sea catchment).

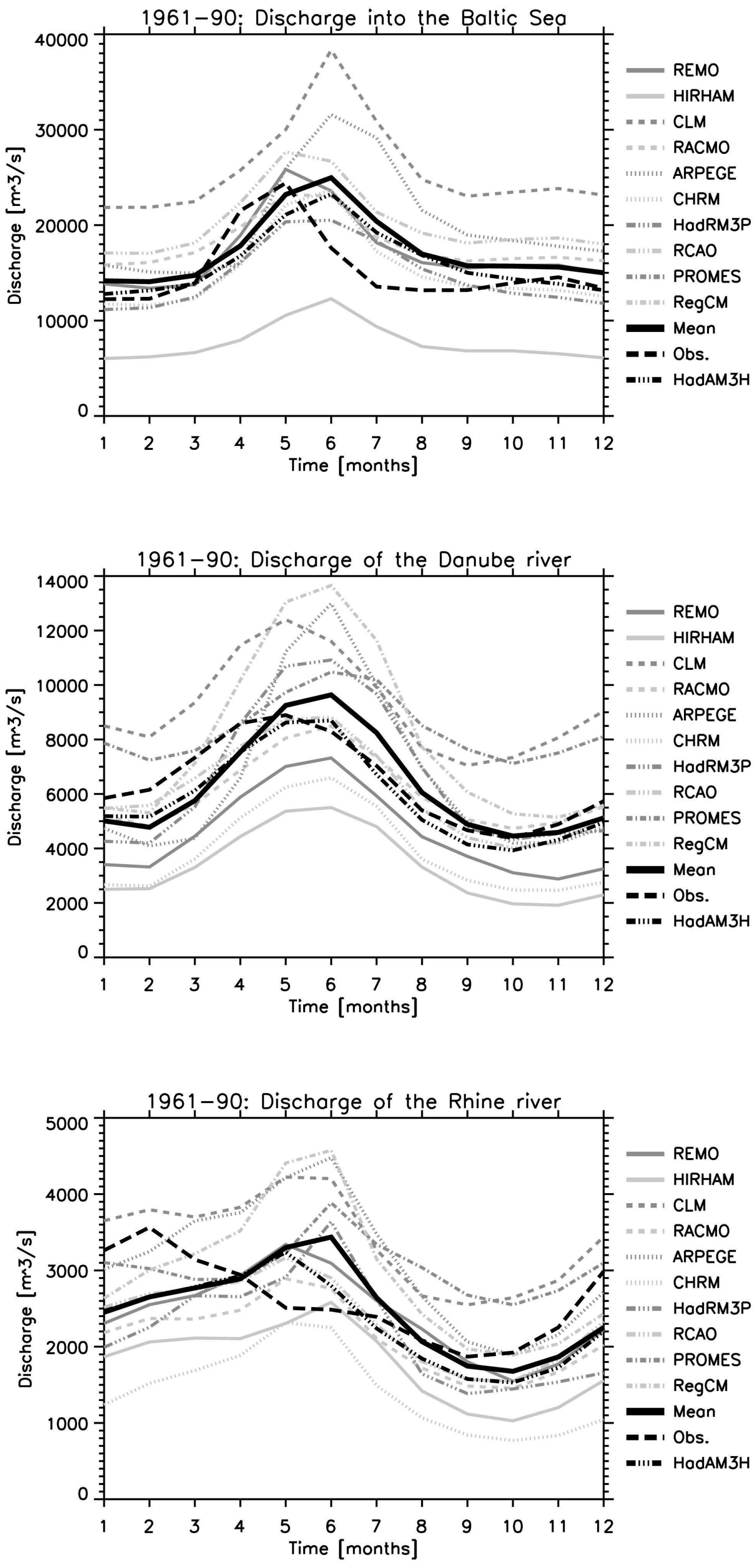

Figure 8 Mean annual cycle of discharge for the a) Baltic Sea catchment, b) Danube and c) Rhine. Mean designates the multi-model ensemble mean of the 10 RCMs (8 for the inflow into the Baltic Sea).

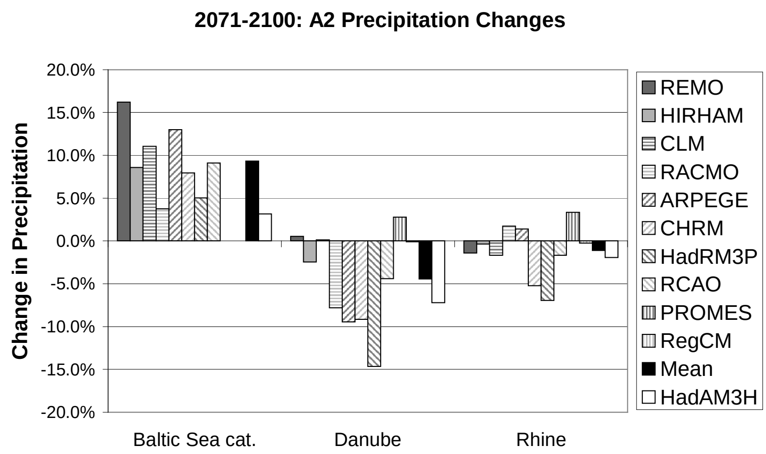

Figure 9 Annual mean changes in precipitation over the catchments of Baltic Sea, Danube and Rhine.

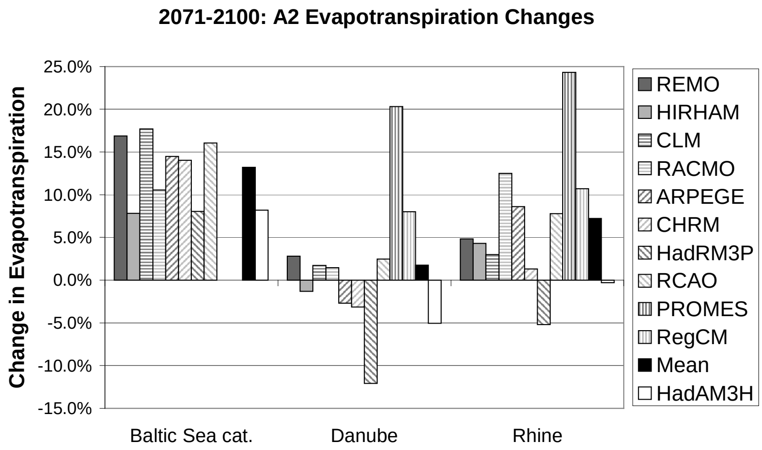

Figure 10 Annual mean changes in evapotranspiration over the catchments of Baltic Sea, Danube and Rhine.

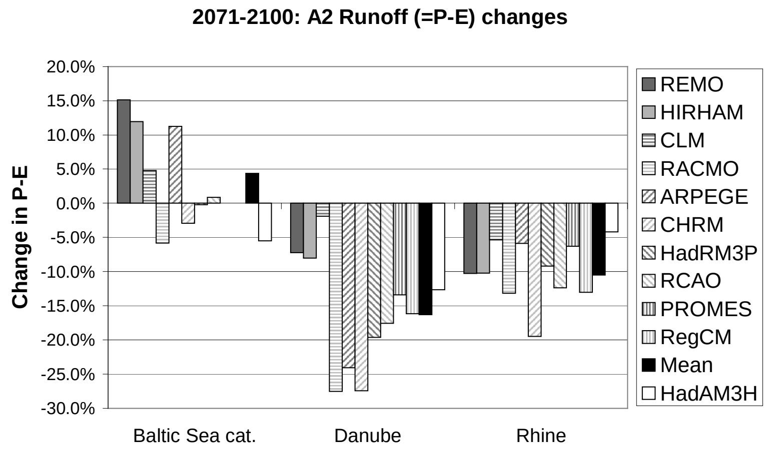

Figure 11 Annual mean changes in P-E (= runoff) over the catchments of Baltic Sea, Danube and Rhine.

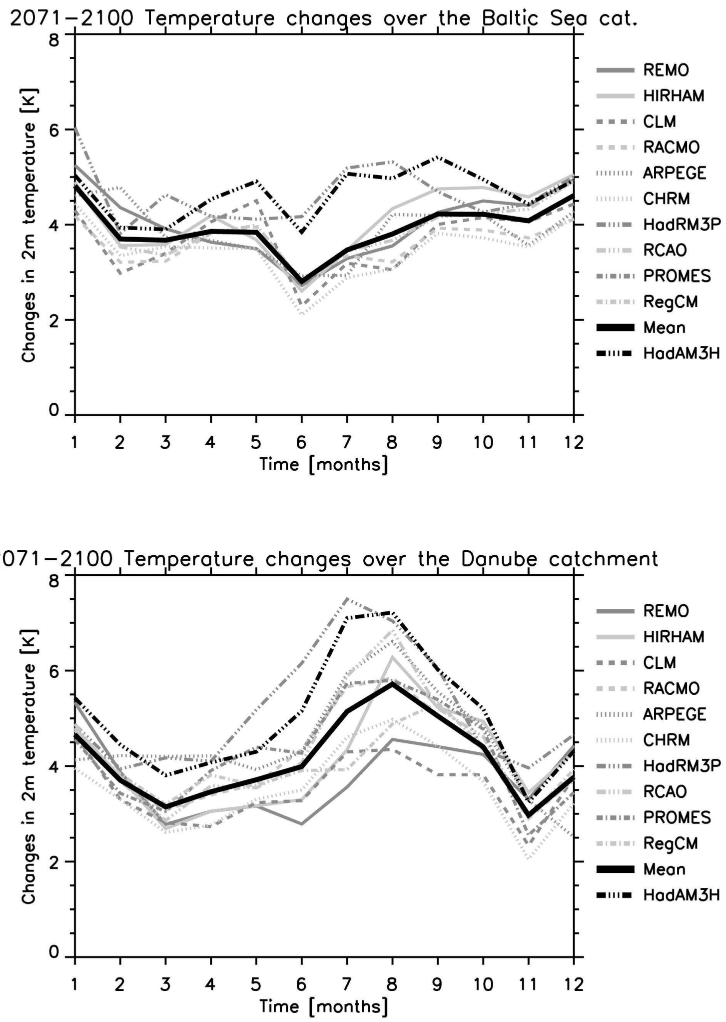

Figure 12 Mean monthly 2m temperature changes over the catchments of a) Baltic Sea and b) Danube. Mean designates the multi-model ensemble mean change of the 10 RCMs (8 for the Baltic Sea catchment).

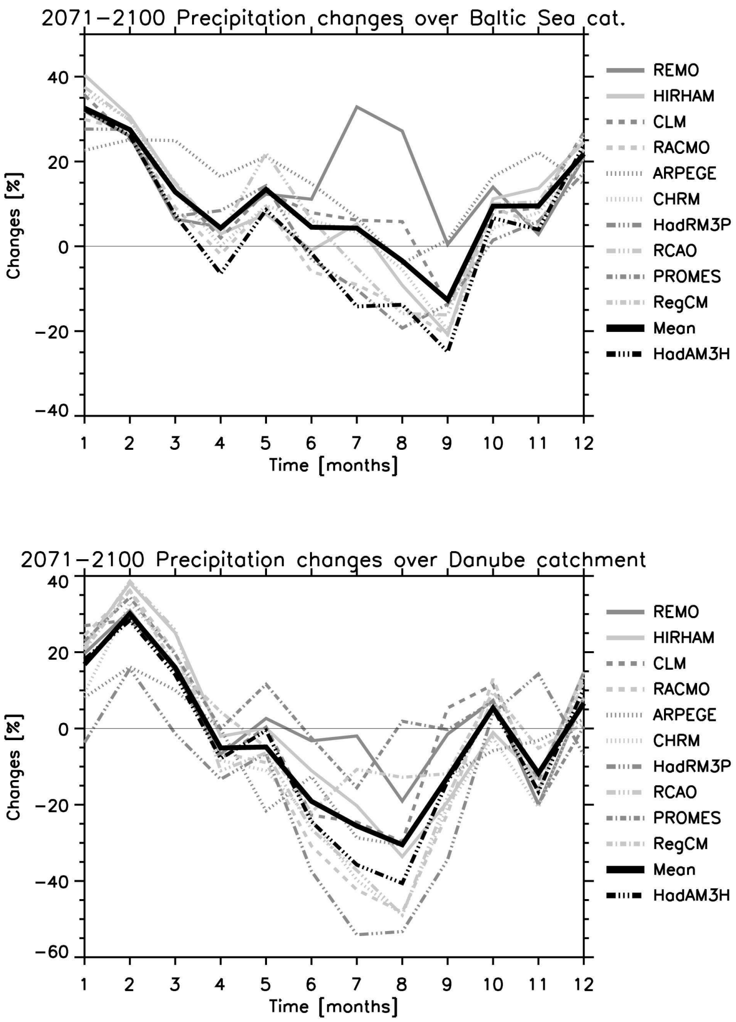

Figure 13 Mean monthly precipitation changes over the catchments of a) Baltic Sea and b) Danube. Mean designates the multi-model ensemble mean change of the 10 RCMs (8 for the Baltic Sea catchment).

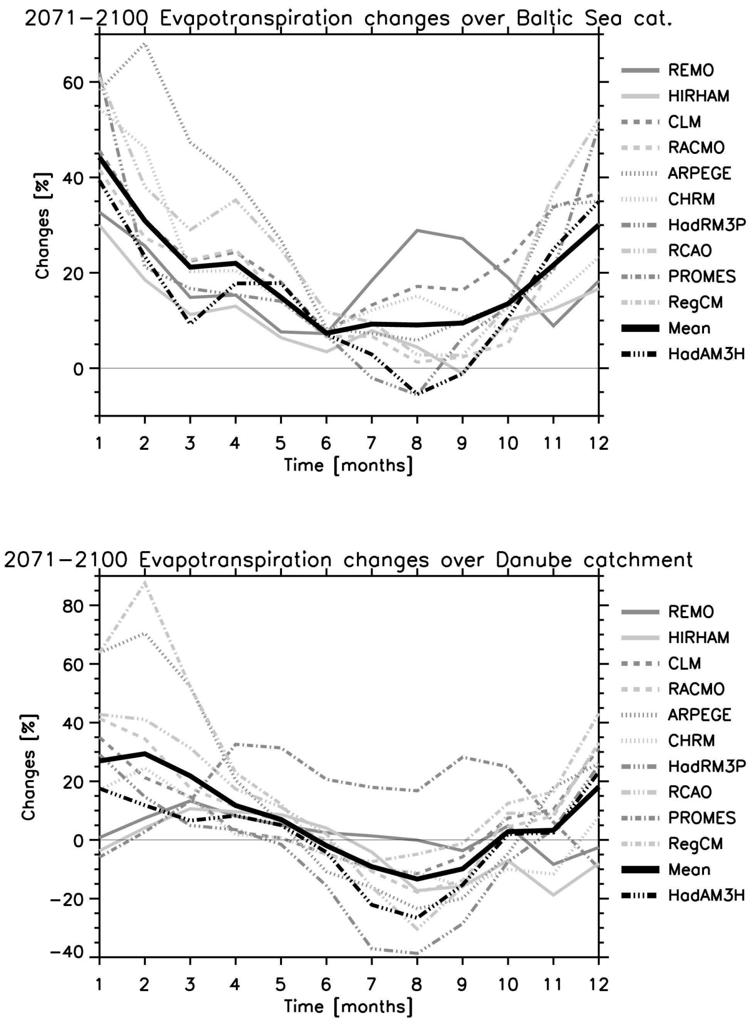

Figure 14 Mean monthly evapotranspiration changes over the catchments of a) Baltic Sea and b) Danube. Mean designates the multi-model ensemble mean change of the 10 RCMs (8 for the Baltic Sea catchment).

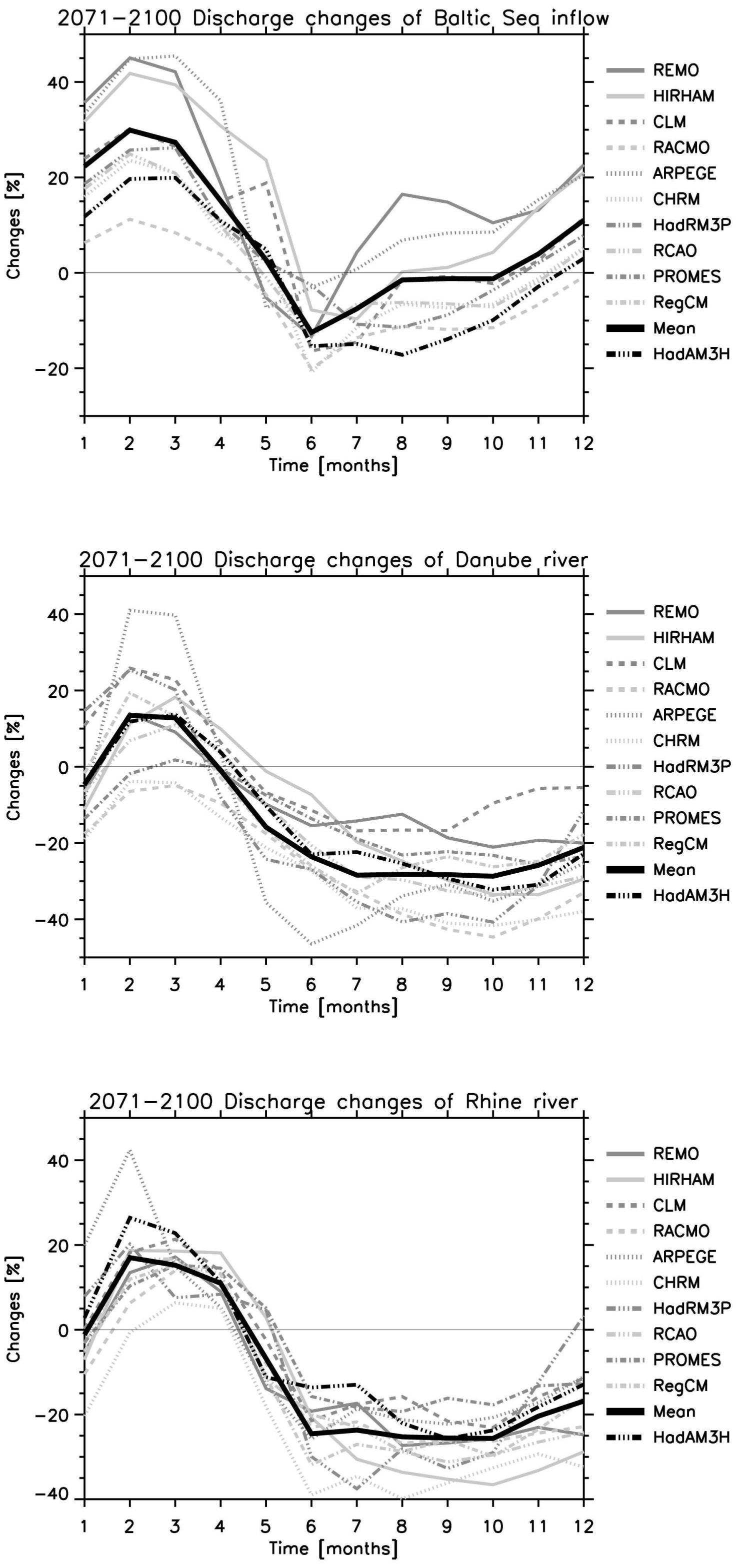

Figure 15 Mean monthly discharge changes in the a) Baltic Sea catchment, b) Danube and c) Rhine. Mean designates the multi-model ensemble mean change of the 10 RCMs (8 for the Baltic Sea catchment).

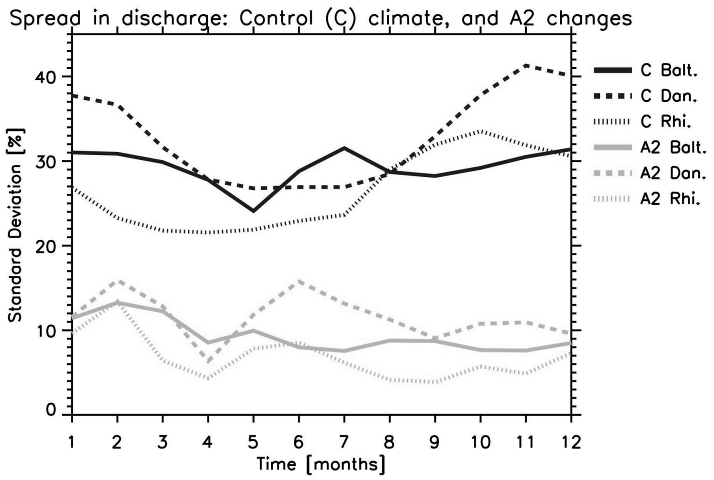

Figure 16 Spread around the multi-model ensemble mean discharge for the control simulations (dark curves) compared to the spread of the predicted discharge changes (pale curves) in the Baltic Sea catchment (solid), the Danube (dashed) and the Rhine (dotted). The spread is given relative to the multi-model ensemble mean discharge.